Experimental Verification of Deep Field Weakening Operation of a 50-kW IPM Machine by Using Single Current Regulator

Yuan Zhang, *Student Member, IEEE*, Longya Xu, *Fellow, IEEE*, Mustafa K. Güven, *Member, IEEE*, Song Chi, *Member, IEEE*, and Mahesh Illindala, *Member, IEEE*

***Abstract*—This paper analyzes critical control issues associated with the deep field weakening operation of interior permanent magnet (IPM) synchronous machines. The single-current-regulator control algorithm is reviewed, which controls the d-axis current actively and gives a fixed q-axis voltage command. To achieve better operational efficiency and performance, improvements are made to choose an optimal q-axis voltage for variable-speed and variable-load conditions. The control algorithm is implemented on a 50-kW IPM machine. Test results, including 7:1 constant power speed ratio operation, are presented to verify the theoretical analysis.**

***Index Terms*—Constant power speed ratio (CPSR), deep field weakening operation, interior permanent magnet (IPM) synchronous machine, single current regulator.**

I. Introduction

INTERIOR permanent magnet (IPM) synchronous machines have attracted great attention in various industry applications, particularly the hybrid electric vehicle technology, for the last couple of decades because of their high power density, good capability of constant power operation in a very wide speed range, fast torque–speed response, and decreasing price of PM materials [1]–[3]. Lately, due to advanced electric machine design methods, an IPM machine system with a much improved constant power speed ratio (CPSR) has been demonstrated. In the demonstrated system, a CPSR as high as 9.5 has been achieved [4]. With substantial progress and achievement in machine design techniques and control theories, IPM machines have become one of the most favorable choices and entered even wider and higher power applications.

Literature review indicates that stable control of IPM machines in the deep field weakening operation region still remains an issue to achieve the largest possible speed range [5]–[7]. Traditional vector control algorithms for IPM machines apply two independent current regulators, i.e., one for the d-axis current regulation and the other for the q-axis current regulation. Good performance can be achieved with well-regulated currents in the constant-torque region and slightly beyond. However, in the deep field weakening operation region, the effects of terminal voltage limitation become serious. Saturation of the two current regulators often occurs when the command voltage is larger than the maximum voltage available. Consequently, the two current regulators conflict with each other, leading to nuisance instability of current and torque of IPM machines. As a result, the theoretical speed range of IPM machines is not attainable.

A solution to stabilizing PM machines in the field weakening operation region was proposed by using the single-current-regulator control algorithm [8], [9]. The proposed algorithm controls the torque and speed of a surface-mounted PM machine by using only the d-axis current regulation and giving a fixed command to the q-axis voltage. The q-axis current is generated automatically in terms of different speeds and torque levels. In previous research work [10], the single-current-regulator algorithm is applied to IPM machine control. Recommendation is also made in choosing an optimal q-axis voltage for variable speeds and torque. However, only computer simulation results and some experimental results below 2000 r/min under no-load conditions were presented.

This paper analyzes the critical issues associated with deep field weakening operation for IPM machines. Then, the control algorithm with a single current regulator is reviewed. The criteria for an optimal q-axis voltage command are demonstrated, and computer simulations are carried out to prove the improvements by applying the optimal q-axis voltage command. The improved single-current-regulator control algorithm is implemented on a heavy-duty traction system using a 50-kW IPM machine. Experimental results, including the 7:1 CPSR operation, under variable-load conditions are presented to substantiate the research work of this paper.

II. Control Algorithm and System Configuration

The voltage equations of an IPM machine in the synchronous reference frame at the steady state can be written as

$$v_d = R_s i_d - \omega_e L_q i_q \tag{1}$$

$$v_q = R_s i_q + \omega_e (\lambda_m + L_d i_d) \tag{2}$$

Manuscript received March 28, 2010; revised May 6, 2010 and May 25, 2010; accepted May 28, 2010. Date of publication November 11, 2010; date of current version January 19, 2011. Paper 2010-IDC-116.R2, presented at the 2009 IEEE Energy Conversion Congress and Exposition, San Jose, CA, September 20–24, and approved for publication in the IEEE TRANSACTIONS ON INDUSTRY APPLICATIONS by the Industrial Drives Committee of the IEEE Industry Applications Society.

Y. Zhang and L. Xu are with The Ohio State University, Columbus, OH 43210 USA (e-mail: zhang.564@osu.edu; xu.12@osu.edu).

M. K. Güven and M. Illindala are with Caterpillar Inc., Peoria, IL 61629 USA (e-mail: guven_mustafa_k@cat.com).

S. Chi is with General Electric, Niskayuna, NY 12309 USA (e-mail: s.chi.36@gmail.com).

Digital Object Identifier 10.1109/TIA.2010.2091478

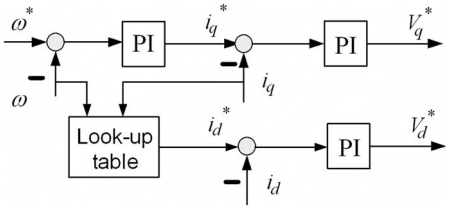

Fig. 1. Traditional current vector control algorithm.

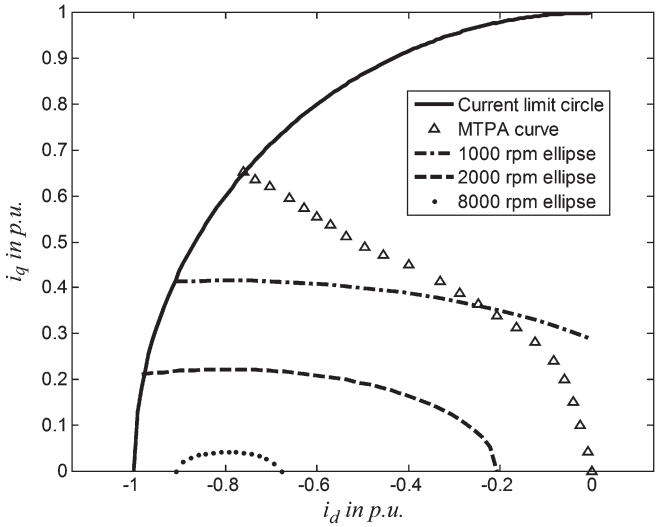

Fig. 2. Operation limit curves in the i_d-i_q plane, showing a critical issue for deep field weakening control of an IPM machine.

where v_d and v_q are the d- and q-axis components of the stator terminal voltage vector, i_d and i_q are the d- and q-axis components of the stator current vector, L_d and L_q are the d- and q-axis components of the armature-winding self-inductance, R_s is the resistance of the stator phase winding, λ_m is the flux linkage produced by the PMs, and ω_e is the electrical angular velocity of the rotor.

A. Critical Control Issues for Deep Field Weakening Operation of IPM Machines

One critical control issue for the field weakening operation of the IPM machine is due to the limited dc bus voltage. Fig. 1 shows the traditional current vector control algorithm for an IPM machine by using two current regulators. In the field weakening operation region, the voltage commands v_d^* and v_q^* may exceed the maximum available voltage, which will cause saturation of current regulators. The saturated regulators will conflict with each other and then result in an unacceptable performance of current, torque, and speed. The operation point of the IPM machine may switch from the motoring mode to the generating mode or vice versa.

Another critical issue for the deep field weakening operation is shown in Fig. 2. Several important operational limit curves and the maximum-torque-per-ampere curve are simultaneously shown in the same i_d-i_q plane.

The machine current should not exceed the allowed maximum value $I_{\max}$, which is constrained by the thermal limits of both the electric machine and the power converter. The current limit is shown in (3) that defines the current limit circle in Fig. 2

$$i_d^2 + i_q^2 \le I_{\max}^2. \tag{3}$$

On the other hand, the terminal voltage of the machine winding should not exceed the maximum voltage $V_{\max}$, which is constrained by the limited dc bus voltage

$$v_d^2 + v_q^2 \le V_{\max}^2. \tag{4}$$

Assume that the resistance of the machine windings is small and the voltage drop across the resistance is negligible compared to the machine back electromotive force (EMF) $\omega_e\lambda_m$. By substituting (1) and (2) into (4), we will get

$$(L_d i_d + \lambda_m)^2 + (L_q i_q)^2 \le \left(\frac{V_{\max}}{\omega_e}\right)^2. \tag{5}$$

The aforementioned equation defines a current limit ellipse imposed by voltage $V_{\max}$ in the i_d-i_q plane. The current limit forms an ellipse instead of a normal circle because of the difference between the d- and q-axis inductances. Equation (5) indicates that the size of the ellipse is speed dependent, and Fig. 2 shows three voltage-imposed limit ellipses at different operation speeds. It is obvious that the size of the current limit ellipse imposed by the voltage decreases rapidly with increasing speed.

Therefore, the possible operation region for a certain speed is constrained by both the current limit circle and the voltage-imposed limit ellipse. When the machine speed is below the base speed, the voltage-imposed limit will never be reached even under full-load conditions. With increasing speed, the size of the voltage-imposed limit ellipse reduces rapidly, resulting in smaller operation regions. Stable operation in the deep field weakening region requires accurately controlled current. The very small operational region implies another critical issue for the high-speed or deep field weakening operation of IPM machines.

B. Single-Current-Regulator Control Algorithm

The q-axis voltage equation (2) can be rewritten as

$$i_q = -\frac{\omega_e L_d}{R_s} i_d + \frac{v_q - \lambda_m \omega_e}{R_s}. \tag{6}$$

When the speed is below the base speed, the back EMF is relatively low, and there is one freedom to choose the control voltage because v_q never reaches the limit. The d- and q-axis currents i_d and i_q can be controlled truly independently. However, when the speed is above the base speed or in the field weakening operation region, v_q is limited by the maximum available dc bus voltage, and i_d and i_q can no longer be regulated independently. In other words, if the control voltage v_q command is fixed, i_q will obey (6) automatically by controlling i_d actively.

Fig. 3 shows the single-current-regulator control algorithm. The speed controller generates the torque command, which is converted into d-axis current command by multiplying a

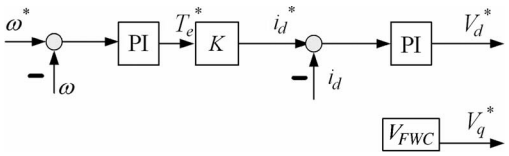

Fig. 3. Single-current-regulator control algorithm.

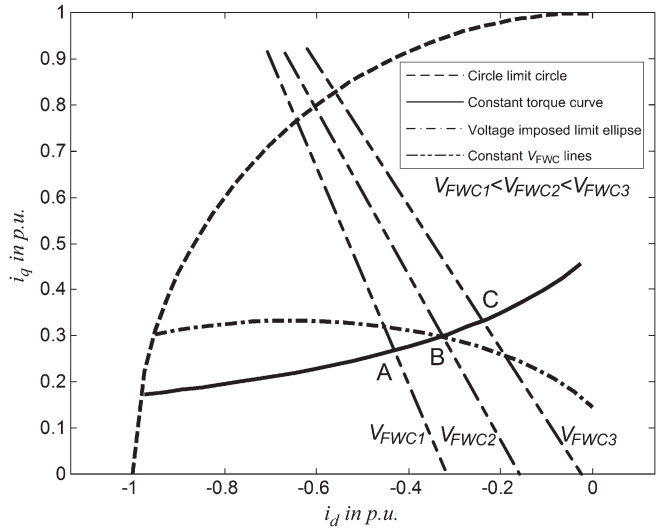

Fig. 4. Optimal V_{FWC} versus speed and torque.

negative constant K simply because the demagnetizing current is always opposed to the flux linkage generated by the PMs. The d-axis current command contains both the demagnetizing current information and the torque information. The output of the d-axis current controller is regarded as the d-axis voltage command. No current control is applied for the q-axis current. Instead, a fixed value is given to the q-axis voltage command. The q-axis current will follow (6) automatically for variable-speed and variable-load conditions. By using the single-current-regulator algorithm, no conflict will occur between the two current regulators anymore, resulting in high system stability even in the deep field weakening operation region.

C. Optimal Control Voltage v_q

In order to achieve better operational efficiency and to fully use the dc bus voltage, an optimal q-axis voltage command is much preferred as mentioned earlier for variable-speed and variable-load conditions. Fig. 4 shows three different values for the q-axis voltage command, where $V_{\mathrm{FWC1}} < V_{\mathrm{FWC2}} < V_{\mathrm{FWC3}}$. The solid curve indicates a constant and desired torque curve of T_e, and the dash-dotted curve is the voltage-imposed limit ellipse at the speed of ω_e. The operation point corresponding to V_{FWC1} (point A) in the i_d–i_q plane is located within the voltage-imposed ellipse which indicates that the terminal phase voltage is still lower than the maximum allowable voltage and the dc bus voltage is not fully used. Operating at point A can satisfy the required speed and torque but at the expense of high current and copper losses. If V_{FWC3} is chosen to be the q-axis voltage, the operation point has to be point C if the torque T_e is required. However, point C is outside the voltage-imposed ellipse at speed ω_e, which means that the desired speed or torque is not achievable. Therefore, V_{FWC1} is a better choice over V_{FWC3}. Compared to V_{FWC1}, V_{FWC2} is even better because not only the dc bus voltage is fully used but also the current and conduction losses to achieve the same amount of desired torque are smaller.

TABLE I
KEY DIMENSIONS AND PARAMETERS FOR THE 50-kW PROTOTYPE IPM MACHINE

Number of poles	8
Stator outer radius	142 mm
Stator inner radius	65.7 mm
Airgap length	0.895 mm
Rotor inner radius	20 mm
Active stack length	322 mm
Rated line-to-line voltage V_R	480 Vrms
Base speed ω_R	850 rpm
Top speed ω_{max}	8000 rpm
Rated torque T_R	562 Nm
Rated phase current I_R	76 Arms

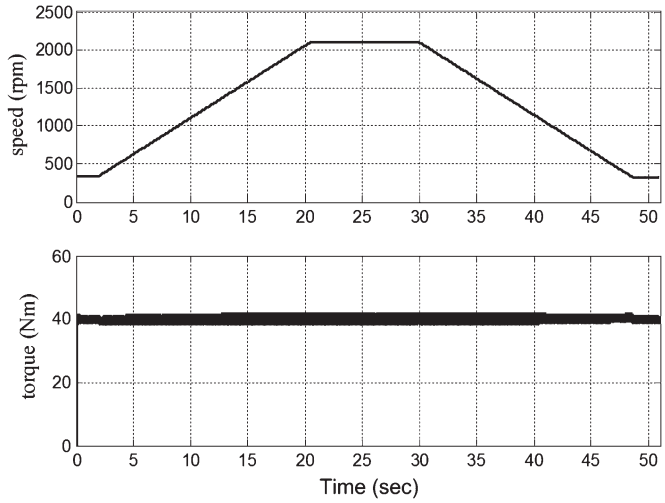

Fig. 5. Speed and torque when the IPM machine runs at a speed with a CPSR of 7:1.

III. SIMULATION RESULTS AND ANALYSIS

Computer simulations have been carried out to show the effects of the selection of different q-axis voltage commands for the same speed and load condition by using the single-current-regulator algorithm. The machine parameters used in the simulations are the same as those of the 50-kW prototype IPM machine. Some important parameters and ratings of the machine are cited directly from [4] and listed in Table I.

In computer simulations, the dc bus voltage is reduced so that the field weakening operation starts from 300 r/min instead of 850 r/min. Fig. 5 shows that the IPM machine accelerates from 300 to 2100 r/min, maintains at 2100 r/min for 10 s, and decelerates again with a constant load of 40 N · m. The simulated field weakening CPSR is 7:1.

First, the q-axis voltage command v_q is always fixed at a constant value for the entire process of acceleration and deceleration in the field weakening operation region. Fig. 6 shows the

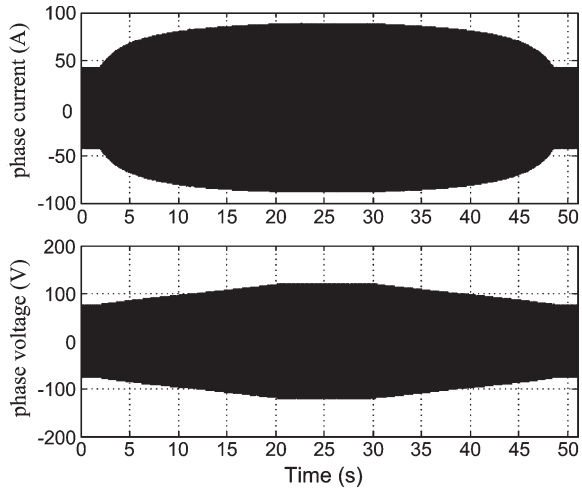

Fig. 6. Phase current and phase voltage by using fixed v_q control.

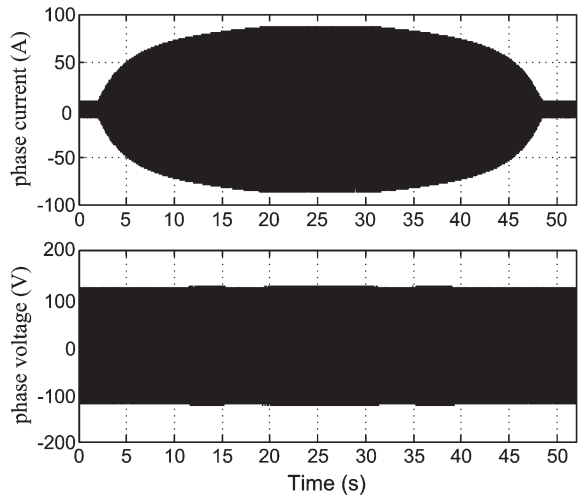

Fig. 7. Phase current and phase voltage by using optimal v_q control.

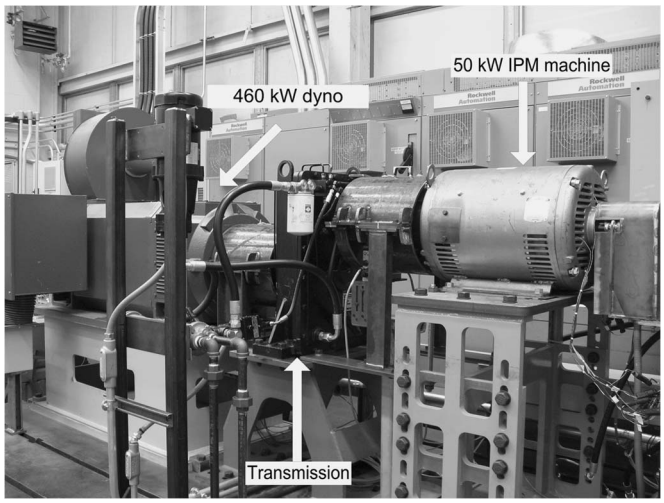

Fig. 8. IPM drive system under test.

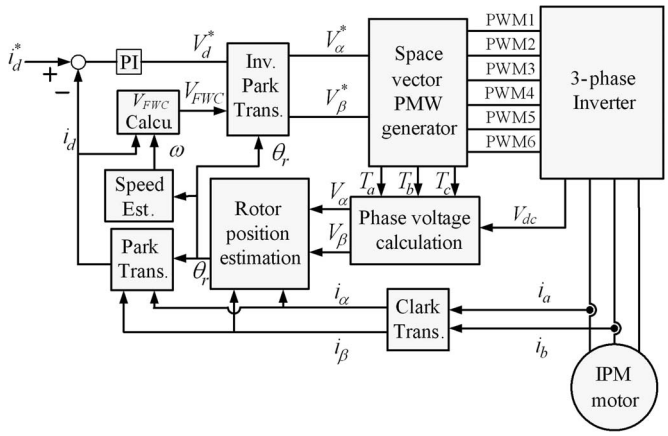

Fig. 9. System control block diagram.

waveforms of the phase current and the phase voltage. Second, the optimal q-axis voltage control adaptive to the variable-speed and variable-load conditions discussed in the previous part is applied to run the machine over the same speed profile and load condition as in the first simulation. The results are shown in Fig. 7.

In Fig. 6, the phase voltage does not reach the maximum level when the machine is accelerating and decelerating, which means that the dc bus voltage is not fully used. In Fig. 7, the phase voltage always maintains at the maximum level for all speeds, which means that the dc bus voltage is always fully utilized. Since the dc bus voltage is not fully used for the fixed q-axis voltage control, as expected, a larger phase current is needed to run the machine at the same speed and load condition. The computer simulation has yielded results strongly supporting the theoretical analysis.

IV. Experimental Results and Analysis

Experiments have been performed on a 50-kW prototype IPM machine by using the improved single-current-regulator control algorithm. Fig. 8 shows the IPM machine drive system under test. A 460-kW induction machine used as a dyno is coupled to the 50-kW IPM machine by a transmission box. The gear ratio between the induction machine and the IPM machine is $2.52:1$. The induction machine is working under torque control mode. Fig. 9 shows the system control block diagram. A current profile is given to the d-axis current command manually instead of using a speed controller. The q-axis voltage command is adjusted automatically in terms of variable speed and load.

Fig. 10 shows the experimental results when the motor accelerates from about 300 to 2000 r/min. In the figure, (a) shows the waveforms of the load torque and speed profiles, and (b) shows the dc bus voltage and phase current. The IPM motor outputs a mechanical power of 49.5 kW at 2000 r/min, which is about 2.4 times the base speed. Fig. 10(c) shows the details of the three-phase current. Fig. 11 shows the experimental results when the IPM motor accelerates from about 300 to 6000 r/min which is seven times the base speed. At 6000 r/min, the mechanical output power of the IPM machine is about 28 kW.

In the deep field weakening operation region, the single-current-regulator algorithm demonstrates its superiority over the conventional two-current-regulator algorithm. By using the single-current-regulator algorithm, the conflict between the two saturated current regulators no longer exists. Repeated tests show that the IPM machine can run in a stable manner even

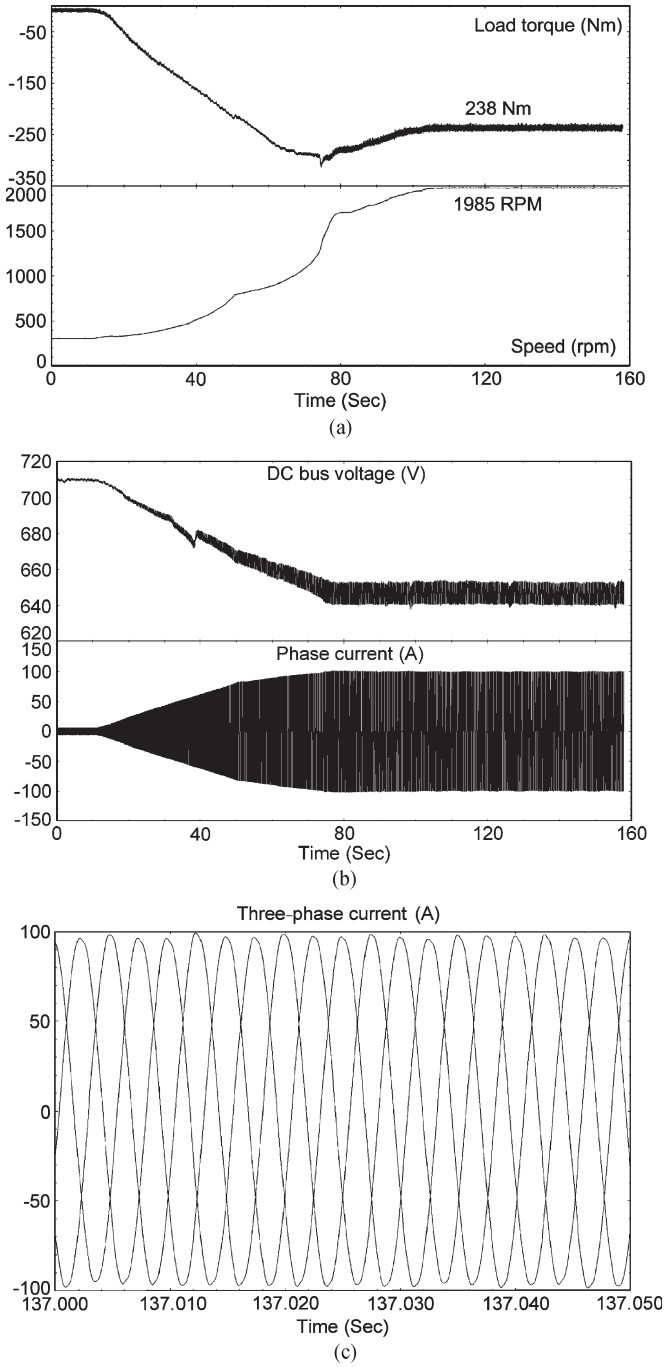

Fig. 10. Experimental results with the motor accelerating to 2000 r/min with full load. (a) Torque and speed. (b) DC bus voltage and phase current. (c) Three-phase current.

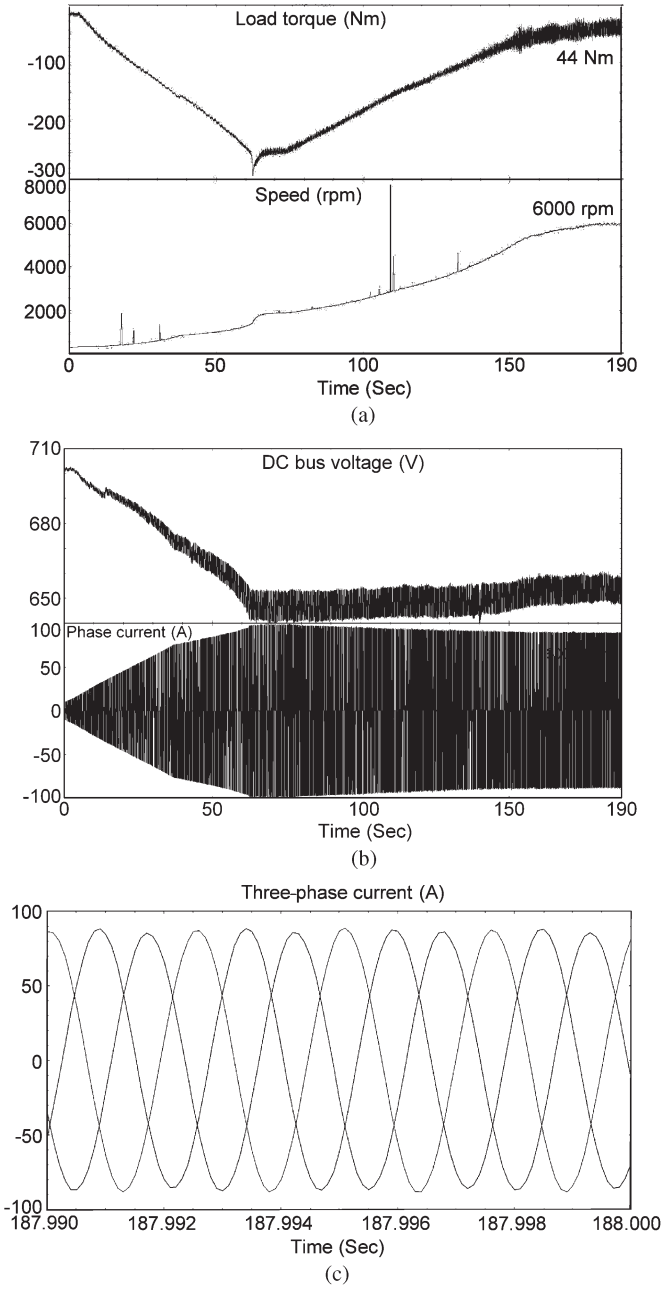

Fig. 11. Experimental results with the motor accelerating to 6000 r/min with 55% load. (a) Torque and speed. (b) DC bus voltage and phase current. (c) Three-phase current.

when the operation region is reduced to a very small ellipse in the i_d–i_q plane.

In the aforementioned experiments, the system accelerates slowly in the field weakening operation region because the total rotating inertia of the IPM machine, the transmission box, and the induction machine is as large as 3.0 kg · m^2. System failures in the deep field weakening operation could cause severe damage to the power converter circuits and even personnel safety issues. Considering the cost and safety of both the high-power system and testing engineers, it was chosen to accelerate the machine slowly so that fast response could be carried out to take care of emergency situations to minimize possible damage to the system.

V. Conclusion

This paper has focused on the control strategies and experimental verification of the deep field weakening operation of IPM machines. The critical control issues of deep field weakening operation of IPM machines have been discussed. Key observations by reviewing the dynamic model of IPM machines include the following.

1) The d- and q-axis currents are strongly coupled and cannot be controlled truly independently in the

field weakening operation region, which is also indicated by the conflict between two current regulators. Therefore, the q-axis current has to obey the machine equation automatically in terms of variable speed and load. The simplest strategy is to fix the q-axis voltage command at a proper value while actively controlling the d-axis current.

2) Selection of the q-axis voltage v_q affects the operational efficiency and performance of the system. Criteria for an optimal q-axis voltage v_q are established by comparison investigation on various choices of voltage for the same operation point.

The single-current-regulator algorithm is realized and tested on a 50-kW prototype IPM machine. The experimentally achieved results include a 7:1 CPSR operation. The single-current-regulator strategy is fully verified. Repeated tests show that the single-current-regulator algorithm is simple and reliable for the wide-speed-range operation of IPM machines under variable-load conditions.

REFERENCES

[1] T. M. Jahns, "Flux-weakening regime operation of an interior permanent-magnet synchronous motor drive," *IEEE Trans. Ind. Appl.*, vol. IA-23, no. 4, pp. 681–689, Jul. 1987.

[2] W. L. Soong and T. J. E. Miller, "Field-weakening performance of brushless synchronous AC motor drives," *Proc. Inst. Elect. Eng.—Elect. Power Appl.*, vol. 141, no. 6, pp. 331–340, Nov. 1994.

[3] K. Muta, M. Yamazaki, and J. Tokieda, "Development of new-generation hybrid system THS II—Drastic improvement of power performance and fuel economy," *SAE Trans.*, vol. 113, pp. 182–192, 2004.

[4] T. M. Jahns, S. Han, A. M. El-Refaie, J. Baek, M. Aydin, M. K. Güven, and W. L. Soong, "Design and experimental verification of a 50 kW interior permanent magnet synchronous machine," in *Conf. Rec. 41st IEEE IAS Annu. Meeting*, Oct. 2006, vol. 4, pp. 1941–1948.

[5] S. Morimoto, M. Sanada, and Y. Takeda, "Wide-speed operation of interior permanent magnet synchronous motors with high-performance current regulator," *IEEE Trans. Ind. Appl.*, vol. 30, no. 4, pp. 920–926, Jul./Aug. 1994.

[6] J. Kim and S. Sul, "Speed control of interior permanent magnet synchronous motor drive for the flux weakening operation," *IEEE Trans. Ind. Appl.*, vol. 33, no. 1, pp. 43–48, Jan./Feb. 1997.

[7] Y. Yoon, W. Lee, and S. Sul, "New flux weakening control for high saliency interior permanent magnet synchronous machine without any tables," in *Proc. IEEE Eur. Conf. Power Electron. Appl.*, 2007, pp. 1–7.

[8] S. Chi, Z. Zhang, and L. Xu, "A robust, efficiency optimized flux-weakening control algorithm for PM synchronous machines," in *Conf. Rec. 42nd IEEE IAS Annu. Meeting*, Sep. 2007, pp. 1308–1314.

[9] S. Chi and L. Xu, "A special flux-weakening control scheme of PMSM-incorporating and adaptive to wide-range speed regulation," in *Proc. 5th IEEE Int. Power Electron. Motion Control Conf.*, Aug. 2006, vol. 2, pp. 1–6.

[10] L. Xu, Y. Zhang, and M. K. Güven, "A new method to optimize q-axis voltage for deep flux weakening control of IPM machines based on single current regulator," in *Proc. IEEE Int. Conf. Elect. Mach. Syst.*, 2008, pp. 2750–2754.

Yuan Zhang (S'07) received the B.S. and M.S. degrees in electrical engineering from Nanjing University of Aeronautics and Astronautics, Nanjing, China, in 2002 and 2005, respectively. She is currently working toward the Ph.D. degree in electrical engineering at The Ohio State University, Columbus.

Her research interests include variable-speed drive control, applications of power electronics, and electric machine design.

Longya Xu (S'89–M'90–SM'93–F'04) received the M.S. and Ph.D. degrees in electrical engineering from the University of Wisconsin, Madison, in 1986 and 1990, respectively.

In 1990, he joined the Department of Electrical Engineering, The Ohio State University, Columbus, where he is currently a Professor and the Director of the newly established Center for High Performance Power Electronics supported by the Ohio Third Frontier Program. He has served as a Consultant to many industrial companies, including Raytheon Company, Boeing, Honeywell, GE Aviation, the U.S. Wind Power Company, General Motors, Ford, and Unique Mobility Inc. His research and teaching interests include dynamic and optimized design of special electrical machines and power converters for variable-speed systems, applications of advanced control theory and digital signal processors for motion control, and distributed power systems in super-high-speed operation. For 20 years, he has conducted many research projects on electrical and hybrid electrical vehicles and variable-speed constant-frequency wind power generation systems.

Dr. Xu was the recipient of the 1990 First Prize Paper Award from the Industrial Drives Committee of the IEEE Industry Applications Society (IAS) and a 1991 Research Initiation Award from the National Science Foundation for wind power generation. He was also a recipient of the 1995, 1999, and 2004 Lumley Research Awards for his outstanding research accomplishments from the College of Engineering, The Ohio State University. He has served as the Chairman of the Electric Machines Committee of the IEEE IAS and an Associate Editor of the IEEE TRANSACTIONS ON POWER ELECTRONICS in the past several years. He is currently a Member-at-Large of the IEEE IAS Executive Board.

Mustafa K. Güven (M'01) received the B.Sc. degree in electrical engineering, specializing in microprocessor-based industrial systems, from Istanbul Technical University, Istanbul, Turkey, in 1993, and the M.S. degree in electrical engineering, specializing in control system theory, and the Ph.D. degree in electrical engineering, specializing in power electronics, electric machines, and drives, from The Ohio State University, Columbus, in 1997 and 2001, respectively.

He is currently with Caterpillar Inc., Peoria, IL. His research interests include advanced control theory, digital signal processors and their applications in controlling motion systems, electric machine design and control, and power electronics.

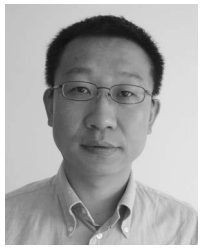

Song Chi (S'04–M'07) received the B.S. degree in electrical engineering from Northeastern University, Shenyang, China, in 1993, the M.S. degree in electrical engineering from Tsinghua University, Beijing, China, in 2000, and the Ph.D. degree in electrical engineering from The Ohio State University, Columbus, in 2007.

He was a Senior Engineer with the Research and Engineering Center of Whirlpool Corporation. He is currently with the Global Research Center, General Electric, Niskayuna, NY. His research interests include sensorless control of ac drives, flux-weakening control of surface/interior permanent magnet machines, and pulse width modulation generation schemes for multilevel inverters.

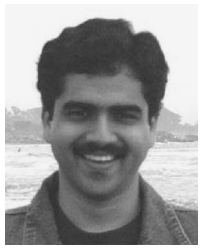

Mahesh Illindala (S'01–M'06) received the B.Tech. degree in electrical engineering from the National Institute of Technology, Calicut, India, in 1995, the M.Sc. (Engg.) degree in electrical engineering from the Indian Institute of Science, Bangalore, India, in 1999, and the Ph.D. degree in electrical engineering from the University of Wisconsin, Madison, in 2005.

Since October 2005, he has been with Caterpillar Inc., Peoria, IL, working on the research, development, and design of power electronics for electric drivetrains and alternative power sources. His research interests include power electronics, electrical energy conversion and storage, and electric drivetrains.